



Published in final edited form as:

J Am Chem Soc. 2017 April 05; 139(13): 4943–4947. doi:10.1021/jacs.7b01269.

Stereochemistry of Endogenous Palmitic Acid Ester of 9-Hydroxystearic Acid and Relevance of Absolute Configuration to Regulation

Andrew T. Nelson^{1,2,3,||}, Matthew J. Kolar^{4,||}, Qian Chu⁴, Ismail Syed⁵, Barbara B. Kahn⁵, Alan Saghatelian⁴, and Dionicio Siegel^{1,*}

¹Skaggs School of Pharmacy and Pharmaceutical Sciences, University of California-San Diego, 9500 Gilman Drive, La Jolla, California 92093-0934, United States

²Department of Chemistry, University of Texas at Austin, 105 E 24th Street, A5300, Austin, TX 78712-1224

³School of Medicine, University of Texas Medical Branch, 301 University Boulevard, Galveston, TX 77555

⁴Clayton Foundation Laboratories for Peptide Biology, Salk Institute for Biological Studies, 10010 North Torrey Pines Road, La Jolla, CA 92037-1002, United States

⁵Division of Endocrinology, Diabetes and Metabolism, Department of Medicine, Beth Israel Deaconess Medical Center, Harvard Medical School, Boston, Massachusetts 02215, United States

Abstract

Lipids have fundamental roles in the structure, energetics, and signaling of cells and organisms. The recent discovery of fatty acid esters of hydroxy fatty acids (FAHFAs), lipids with potent anti-diabetic and anti-inflammatory activities, indicates that our understanding of the composition of lipidome and the function of lipids is incomplete. The ability to synthesize and test FAHFAs was critical in elucidating the roles of these lipids, but these studies were performed with racemic mixtures, and the role of stereochemistry remains unexplored. Here, we synthesized the *R*- and *S*-palmitic acid ester of 9-hydroxystearic acid (*R*-9-PAHSA, *S*-9-PAHSA). Access to highly enantioenriched PAHSAs enabled the development of a liquid chromatography-mass spectrometry (LC-MS) method to separate and quantify *R*- and *S*-9-PAHSA, and this approach identified *R*-9-PAHSA as the predominant stereoisomer that accumulates in adipose tissues from transgenic mice where FAHFAs were first discovered. Furthermore, biochemical analysis of 9-PAHSA biosynthesis and degradation indicate that the enzymes and pathways for PAHSA production are stereospecific, with cell lines favoring the production of *R*-9-PAHSA and carboxyl ester lipase (CEL), a PAHSA degradative enzyme, selectively hydrolyzing *S*-9-PAHSA. These studies highlight the role of stereochemistry in the production and degradation of PAHSAs and define the

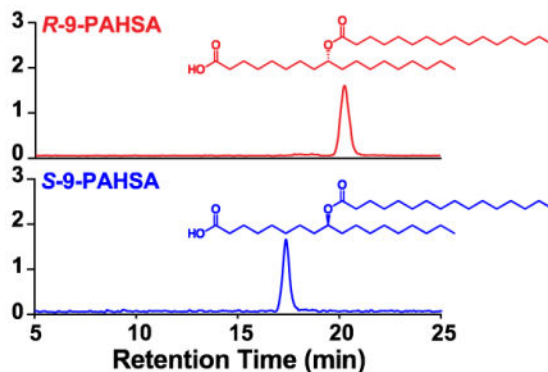
*Corresponding Author: drsiegel@ucsd.edu.

||A.T.N and M.J.K. contributed equally.

Supporting Information. The Supporting Information is available free of charge via the Internet at <http://pubs.acs.org>. Detailed description of synthetic procedures for nonracemic 9-PAHSA, characterization data, and spectra is available. Analytical and biological assay procedures are provided.

endogenous stereochemistry of 9-PAHSA in adipose tissue. This information will be useful in the identification and characterization of the pathway responsible for PAHSA biosynthesis, and access to enantiopure PAHSAs will elucidate the role of stereochemistry in PAHSA activity and metabolism *in vivo*.

Graphical abstract



INTRODUCTION

Mice engineered to overexpress the glucose transporter, GLUT4, selectively in their adipose tissue (AG4OX mice)¹⁻³ have provided insights into the link between obesity and Type 2 diabetes because they are obese but have lower fasting glycemia and enhanced glucose tolerance. Analysis of adipose tissues from AG4OX mice demonstrated marked increases in *de novo* lipogenesis,²⁻³ and this activity is necessary for the enhanced glucose tolerance in these animals. Lipidomics analysis of adipose tissue from AG4OX mice to identify specific lipids that might contribute to the insulin sensitive phenotype led to the discovery of a novel class of lipids⁴ that are highly elevated in AG4OX adipose tissues.⁴ These lipids were named Fatty Acid esters of Hydroxy Fatty Acids (FAHFAs) to describe their structures (Figure 1).

FAHFAs contain two acyl chains connected through a single ester bond (Figure 1), and further targeted liquid chromatography-mass spectrometry (LC-MS) determined that at least 16 different FAHFA families exist,⁴ which differ in their acyl chain constituents (Figure 1), and additional FAHFA families have been found since.⁵⁻⁶ For instance, palmitic acid esters of hydroxy stearic acids (PAHSAs) and oleic acid esters of hydroxy stearic acid (OAHSAs) are two of the most abundant families that were identified.⁴ In addition, for each FAHFA family that has been looked at in detail, different ester regioisomers exist (Figure 1). In adipose tissue of wild-type and AG4OX mice, eight distinct PAHSA regioisomers (5, 7, 8, 9, 10, 11, 12, and 13) were identified.⁴ Regioisomers demonstrate differential regulation and biological activity. For example, all the PAHSA regioisomers were markedly elevated in adipose tissue and serum of AG4OX mice while the isomers in liver were decreased. Furthermore, when wild type mice were placed on a high-fat diet, only two PAHSA isomers were changed in serum, while all isomers were reduced in subcutaneous adipose tissue but some were elevated in perigonadal adipose tissue⁴. This suggests that PAHSAs can be regulated as a family or individually under different conditions and in different tissues.

Furthermore, 5- and 9-PAHSA have potent anti-diabetic effects *in vivo* and enhance glucose transport and insulin secretion *in vitro*, but only 9-PAHSA has anti-inflammatory effects in dendritic cells, highlighting regiospecific biological activity.⁴

Interest in the PAHSAs was piqued further by the analysis of human sera that revealed that PAHSA levels are lower in insulin-resistant humans relative to their insulin-sensitive counterparts, suggesting that PAHSAs may play an important role in maintaining normal blood sugar and insulin sensitivity in people.⁴ In-deed, oral administration of 9-PAHSA or 5-PAHSA to mice on a high-fat diet improved glucose tolerance through multiple pathways that include increases in glucagon-like peptide 1 (GLP-1) and insulin secretion.⁴

The anti-inflammatory properties of FAHFAs can also extend to the treatment of inflammatory diseases as was demonstrated by recent work showing that oral 9-PAHSA treatment reduces the severity and impedes inflammation and damage associated with colitis in a mouse model.⁷ And other novel FAHFA families with anti-inflammatory activities have recently been discovered. Omega-3 fatty acid FAHFAs, produced after the addition of omega-3-fatty acids to cells, have potent anti-inflammatory activity.⁵

Thus, FAHFAs, and in particular PAHSAs, are an exciting class of novel lipids with a range of biological activities. One important structural question that remains unanswered is the natural configuration of the chiral center in PAHSAs. We studied 9-PAHSA, the most abundant and a biologically active PAHSA. Herein we report the first asymmetric synthesis of *R*- and *S*-9-PAHSA (Figure 2) and *R*- and *S*-9-HSA, and utilize these compounds to define the stereochemistry of endogenous 9-PAHSA from AG4OX mouse adipose tissue. This work represents a critical step in understanding PAHSA biology by defining endogenous FAHFA structure.

RESULTS AND DISCUSSION

Synthesis of enantiopure *R*- and *S*-9-PAHSA and 9-HSA

We developed multi-gram scale syntheses of enantiopure *R*- and *S*-9-PAHSA and HSA to further understand the influence of FAHFA structure on their pronounced biological effects. Building upon previous work synthesizing related compounds such as palmitic acid esters of hydroxy palmitic acid (PAHPAs)⁸ and methods for accessing enantioenriched 9-HSA (54% ee)⁹ we have developed a route that provides material on large scale (> 5 gram batches), high enantiomeric excess (>98% ee), and free from heavy metal impurities - all enabling extensive biological testing.

Using epichlorohydrin as both a readily available chiral starting material and lynchpin that connects the three regions of PAHSAs, the synthesis of both enantiomers was achieved. The synthesis of *R*-9-PAHSA (**1-R**) began with the addition of 7-octenylmagnesium bromide into *S*-(+)-epichlorohydrin **4** using catalytic copper (I) iodide to generate chlorohydrin **5** (Scheme 1). Epoxide formation from chlorohydrin **5**, yielding epoxide **6**, was followed by a second epoxide opening reaction at the less substituted position using octylmagnesium chloride in the presence of cuprous iodide to afford secondary alcohol **7** as a solid. The relay of enantiopurity, and retention of configuration at the chiral center, was assessed by

derivatization of **7** as the *S*-O-acetylmandelate ester^{9–10} with the diastereomeric ratio found to be greater than 99:1 (supporting info). Palmitoylation of alcohol **7** with palmitoyl chloride and pyridine provided ester **8**. Reaction of **8** with ozone in the presence of *N*-methylmorpholine *N*-oxide (NMO)¹¹ followed by Pinnick oxidation¹² of the crude intermediate provided *R*-9-PAHSA (**1-R**) in 55% yield. Degradation of *R*-9-PAHSA (**1-R**) by saponification yielded *R*-9-HSA (Supporting Information). *S*-9-PAHSA (**1-S**) and *S*-9-HSA were synthesized in an analogous manner, substituting *R*(+)-epichlorohydrin **9** at the start of the synthesis (in place of *S*(+)-epichlorohydrin **4**) through the same 5 step sequence in 61% overall yield (Scheme 1).

Determination of Endogenous 9-PAHSA Stereochemistry

Fatty acid oxidation is a common event in the production of bioactive lipids. Prostaglandins and leukotrienes, for example, are generated from the oxidation of arachidonic acids.¹³ The enzymatic introduction of oxygen occurs in a stereospecific manner and the stereochemistry in these lipids define their activity.¹⁴ The PAHSAs also contain an oxidized fatty acid, the HSA, which places a stereocenter in this lipid. Since stereochemistry has an important role in bioactive lipid function, and can provide information about the enzymes and biochemical pathways for lipid metabolism, we sought to define the endogenous stereochemistry of 9-PAHSA.

We have an established method to separate and analyze these different families and isomers using reversed-phase chromatography,¹⁵ however, this method is unable to resolve stereoisomers. The first step in determining the stereochemistry of natural FAHFAs required us to develop a method capable of separating the different isomers. We attempted several approaches to separate PAHSAs (Supporting information, **Scheme S1**). First, we used chiral GC, where **1-R** and **1-S** were converted to the corresponding methyl ester using TMS-diazomethane, but we were unable to separate these stereoisomers. Next, we converted **rac-1** to the corresponding amide with *S*-1-phenylethan-1-amine to generate diastereomers that we hoped to separate. These attempts were also unsuccessful, likely owing to the large distance between to two chiral centers.

Unable to separate the 9-PAHSA stereoisomers with our resources, we decided to use Phenomenex's (Torrance, CA) chiral screening service. We provided enantiopure *R*-9-PAHSA and *rac*-9-PAHSA. These compounds were tested on 6 of their chiral columns (Cellulose-1, Cellulose-2, Cellulose-3, Cellulose-4, Amylose-2, and Amylose-1) using 3 different mobile phases (water/acetonitrile, hexane/ethanol, and methanol/isopropanol). The column and mobile phase that provided the best resolution was the Lux 5 μ m Cellulose-3 column with methanol/isopropanol/trifluoroacetic acid (TFA) (90:10:0.1) (Supporting Info, **Figure S1**). Using these conditions and column as a starting point, we continued to refine the method for our purposes. Specifically, we needed to modify the method since TFA is not compatible with LC-MS,¹⁶ and we needed the sensitivity of mass spectrometry to be able to detect 9-PAHSA from endogenous sources.

These efforts led to an optimized method that uses a Lux 3 μ m Cellulose-3 column in combination with an isocratic MeOH/H₂O/formic acid (96:4:0.1) mobile phase (Figure 3A).

Under these conditions, *R*-9-PAHSA elutes from the column at 20.2 min, while *S*-9-PAHSA elutes at 17.4 min, affording 2.8 min of peak separation to resolve these stereoisomers. One caveat with this method is that liquid chromatography conditions required to separate the stereoisomers use formic acid, a mobile phase modifier typically reserved for positive mode ionization, but 9-PAHSA detection by mass spectrometry requires negative mode ionization. In our initial tests we used a mobile phase that was similar to our established FAHFA measurement method, which includes 0.01% ammonium hydroxide,¹⁵ however, this could not achieve base-line resolution of the stereoisomers (Supporting Info, **Fig S2**). It is important to note that with the presence of 0.1% formic acid, we observed a 25-fold reduction in the sensitivity of our detection due to the impaired ionization of the 9-PAHSA (Supporting Info, **Fig S2**). As a result, any possibility of detecting endogenous 9-PAHSA requires a sample with high concentrations of this lipid.

We have previously shown that FAHFA levels are dramatically upregulated in AG4OX mice.³ Specifically, 9-PAHSA levels were elevated ~16–18 fold in the white adipose tissue (WAT) of AG4OX and the final concentration of 9-PAHSA is ~1000pmol/g in perigonadal white adipose tissue (PGWAT). The high 9-PAHSA concentrations make the PGWAT from AG4OX mice the best tissue to measure endogenous 9-PAHSA under conditions of reduced sensitivity. Additionally, by comparing WT and AG4OX samples by chiral LC-MS we can readily identify the 9-PAHSA peak as the one with the largest fold change between the two samples to provide an unambiguous identification of this lipid in the resulting chromatograms. LC-MS analysis of the samples revealed that *R*-9-PAHSA was elevated in AG4OX samples compared to WT PGWAT, with the *R*-9-PAHSA peak clearly elevated in the LC-MS chromatogram (Figure 3A). There is also a much smaller peak that overlaps with the *S*-9-PAHSA standard. We cannot determine if this is *S*-9-PAHSA or a 10-PAHSA stereoisomers because *S*-9-PAHSA or a 10-PAHSA have similar retention times (Supporting Information, **Fig. S3**). We analyzed these same samples using our standard (i.e. non-chiral reverse phase) method (Supporting Info, **Fig. S4**) and found an equivalent fold change for *R*-9-PAHSA (chiral column) and total 9-PAHSA (reversed-phase column) (Figure 3B) highlighting that *R*-9-PAHSA is the main source of the elevated 9-PAHSA levels we observe in AG4OX PGWAT.

Stereospecificity of 9-PAHSA degradation and biosynthesis

Having identified the predominant stereoisomer in AG4OX PGWAT, we wanted to test whether the biochemical pathways or enzymes that control 9-PAHSA biosynthesis and degradation are stereospecific. We have recently identified the enzyme carboxyl ester lipase (CEL) to be a FAHFA hydrolase.¹⁷ CEL is an enzyme of the exocrine pancreas and is secreted into the gut to assist with the digestion of lipids from the diet.¹⁸ Though originally identified as a triglyceride and cholesterol ester hydrolase, our recent work clearly shows that this enzyme prefers FAHFAs, including 9-PAHSA.

The pancreas has the highest 9-PAHSA hydrolytic activity compared to other tissues, and we showed that this FAHFA degrading activity is due to CEL. To determine if CEL prefers *R*- or *S*-9-PAHSA, we carried out a previously reported LC-MS assay to measure hydrolytic activity.^{17, 19} We expressed CEL in HEK293T cells and isolated membrane lysates from

these cells to measure CEL-mediated 9-PAHSA hydrolysis. The data clearly demonstrate that CEL prefers *S*-9-PAHSA to *R*-9-PAHSA as a substrate (Figure 4A), indicating that the enzyme is stereoselective. In support of this finding, this same trend was also observed when testing the hydrolytic activity of these enantiomers in mouse pancreatic membrane lysate (Figure 4B). This data supports the idea that PAHSA metabolism *in vivo* is stereoselective, and at least in the pancreas, this activity favors the degradation of *S*-9-PAHSA.

Although the biosynthetic enzymes responsible for FAHFA synthesis are unknown, it has been previously shown that the addition of palmitoyl-CoA and 9-HSA to liver and WAT lysate results in the production of 9-PAHSA.⁴ Here, we present a cell-based assay where the addition of HSAs results in the production of FAHFAs, such as 9-PAHSA. In this assay, we treat HEK293T cells with either *R*- or *S*-9-HSA, incubate the cells for two hours, and then harvest the cells and extract the 9-PAHSA for subsequent analysis by LC-MS. The *R*- or *S*-9-HSA is acylated by endogenous free fatty acids such as palmitate and oleate, as these were not added as acyl-donors. *R*-9-HSA-treated cells exhibited a substantial increase of 9-PAHSA and 9-OAHSA (~80%) compared to *S*-9-HSA-treated cells (Figure 5). The stereospecificity of 9-PAHSA biosynthesis supports the idea of that PAHSA biosynthesis is mediated by an unidentified acyl transferase and is not the result of a non-enzymatic acylation. Furthermore, these preliminary data indicate a preference for the biosynthesis of *R*-9-PAHSA, which, if similar in adipose tissue could explain the observation of *R*-9-PAHSA as the preferred stereoisomer *in vivo*.

CONCLUSION

The importance of absolute structure in the biochemistry and biological activity of lipids prompted us to develop the first stereoselective synthesis of PAHSAs, which enabled us to identify the natural isomer in adipose tissue as *R*-9-PAHSA. Starting from this important finding, this chemistry will enable access to numerous enantiopure FAHFAs, necessary to better understand their chemistry and biology. As the synthetic approach is modular, it is readily adaptable to the synthesis of related compounds. With the improved sensitivity of our chiral LC-MS method the measurement of additional FAHFA stereoisomers in other tissues is possible.

An important insight from the current work is that FAHFAs are products of enzymatic, not chemical production of the hydroxylated acids. Chemical oxidation of lipids with reactive oxygen species, such as peroxides, results in the production of racemic fatty acids.²⁰ By contrast, enzyme-mediated hydroxy fatty acid production proceeds stereospecifically to produce enantiopure hydroxy lipids.²⁰⁻²¹ The discovery that *R*-9-PAHSA, but not *S*-9-PAHSA, is increasing in the AG4OX WAT supports the idea that this is an enzyme-mediated pathway and chemical oxidation of lipids does not have a role in PAHSA production in these mice. Additional work will endeavor to identify the enzymes and pathways that mediate PAHSA production *in vivo*, and small molecule activators or inhibitors of these PAHSA biosynthetic enzymes might someday allow control over endogenous PAHSAs levels. The continued interplay between chemical synthesis, biology, and bio-chemistry will reveal the biological potential of FAHFAs and identify new ways to regulate these molecules for therapeutic benefit.

Supplementary Material

Refer to Web version on PubMed Central for supplementary material.

Acknowledgments

This work was supported by the National Institutes of Health Grants R01 DK043051 and P30DK57521 (to B. B. K.) and R01 DK106210 (to B. B. K. and A. S.), a grant from the JPB Foundation (to B. B. K.), Leona M. and Harry B. Helmsley Charitable Trust Grant 2012-PG-MED002 (to A. S.), F30 DK112622 (A.T.N.) and F30 DK112604 (M.J.K.), the NCI Cancer Center Support Grant P30 (CA014195 MASS core, A.S.), and Dr. Frederick Paulsen Chair/Ferring Pharmaceuticals (A.S.).

ABBREVIATIONS

FAHFA	fatty acid ester of hydroxy fatty acid
PAHSA	palmitic acid ester of hydroxy stearic acid
HSA	hydroxystearic acid

References

1. Shepherd PR, Gnudi L, Tozzo E, Yang H, Leach F, Kahn BB. *J Biol Chem.* 1993; 268(30):22243–6. [PubMed: 8226728]
2. Tozzo E, Shepherd PR, Gnudi L, Kahn BB. *Am J Physiol.* 1995; 268(5 Pt 1):E956–64. [PubMed: 7762651]
3. Herman MA, Peroni OD, Villoria J, Schon MR, Abumrad NA, Bluher M, Klein S, Kahn BB. *Nature.* 2012; 484(7394):333–8. [PubMed: 22466288]
4. Yore MM, Syed I, Moraes-Vieira PM, Zhang T, Herman MA, Homan EA, Patel RT, Lee J, Chen S, Peroni OD, Dhaneshwar AS, Hammarstedt A, Smith U, McGraw TE, Saghatelian A, Kahn BB. *Cell.* 2014; 159(2):318–32. [PubMed: 25303528]
5. Kuda O, Brezinova M, Rombaldova M, Slavikova B, Posta M, Beier P, Janovska P, Veleba J, Kopecky J Jr, Kudova E, Pelikanova T, Kopecky J. *Diabetes.* 2016; 65(9):2580–90. [PubMed: 27313314]
6. Ma Y, Kind T, Vaniya A, Gennity I, Fahrman JF, Fiehn O. *J Cheminform.* 2015; 7:53. [PubMed: 26579213]
7. Lee J, Moraes-Vieira PM, Castoldi A, Aryal P, Yee EU, Vickers C, Parnas O, Donaldson CJ, Saghatelian A, Kahn BB. *J Biol Chem.* 2016; 291(42):22207–22217. [PubMed: 27573241]
8. Balas L, Bertrand-Michel J, Viars F, Faugere J, Lefort C, CaspaR-Bauguil S, Langin D, Durand T. *Org Biomol Chem.* 2016; 14(38):9012–20. [PubMed: 27603797]
9. Ebert C, Felluga F, Forzato C, Foscatto M, Gardossi L, Nitti P, Pitacco G, Boga C, Caruana P, Micheletti G. *J Mol Cat B: Enzy.* 2012; 83:38–45.
10. Yang W, Dostal L, Rosazza JP. *App Environ Micro.* 1993; 59(1):281–284.
11. Schwartz C, Raible J, Mott K, Dussault PH. *Org Lett.* 2006; 8(15):3199–3201. [PubMed: 16836365]
12. Bal BS, Childers WE, Pinnick HW. *Tetrahedron.* 1981; 37(11):2091–2096.
13. Funk CD. *Science.* 2001; 294(5548):1871–1875. [PubMed: 11729303]
14. Corey E, Marfat A, Goto G, Brion F. *J Am Chem Soc.* 1980; 102(27):7984–7985.
15. Zhang T, Chen S, Syed I, Ståhlman M, Kolar MJ, Homan EA, Chu Q, Smith U, Borén J, Kahn BB. *Nat Protocols.* 2016; 11(4):747–763. [PubMed: 26985573]
16. Gar 1a M, Hogenboom A, Zappey H, Irth H. *J Chrom A.* 2002; 957(2):187–199.
17. Kolar MJ, Kamat SS, Parsons WH, Homan EA, Maher T, Peroni OD, Syed I, Fjeld K, Molven A, Kahn BB. *Biochem.* 2016; 55(33):4636–4641. [PubMed: 27509211]

18. Chen Q, Sternby B, Nilsson Å. *Biochimica et Biophysica Acta (BBA)-Lipids and Lipid Metabolism*. 1989; 1004(3):372–385. [PubMed: 2503032]
19. Parsons WH, Kolar MJ, Kamat SS, Cognetta AB III, Hulce JJ, Saez E, Kahn BB, Saghatelian A, Cravatt BF. *Nat Chem Bio*. 2016; 12(5):367–372. [PubMed: 27018888]
20. Niki E, Yoshida Y, Saito Y, Noguchi N. *Biochem Biophys Res Commun*. 2005; 338(1):668–676. [PubMed: 16126168]
21. Schneider C, Pratt DA, Porter NA, Brash AR. *Chem Bio*. 2007; 14(5):473–488. [PubMed: 17524979]

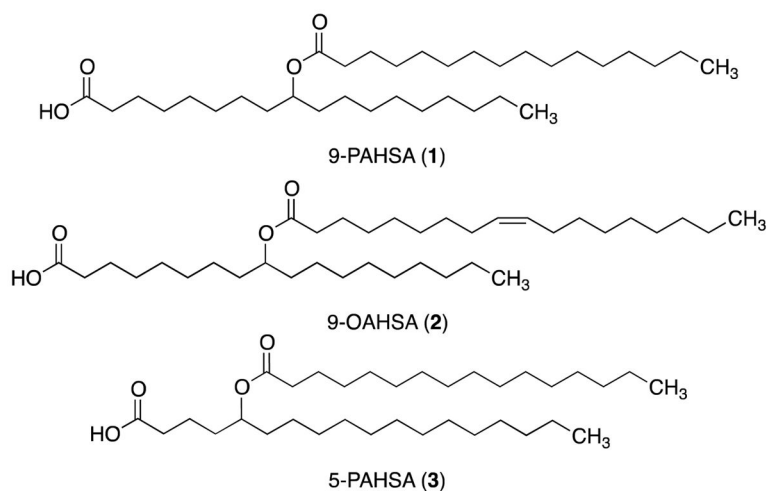


Figure 1. Endogenous FAHFA structures. Analysis of AG4OX mice revealed the existence of FAHFAs. Sixteen different FAHFA families, which differ in the composition of their acyl chains (e.g. PAHSA and OAHSA) were observed. And within each family there exist multiple regioisomers such as 9- and 5-PAHSA.

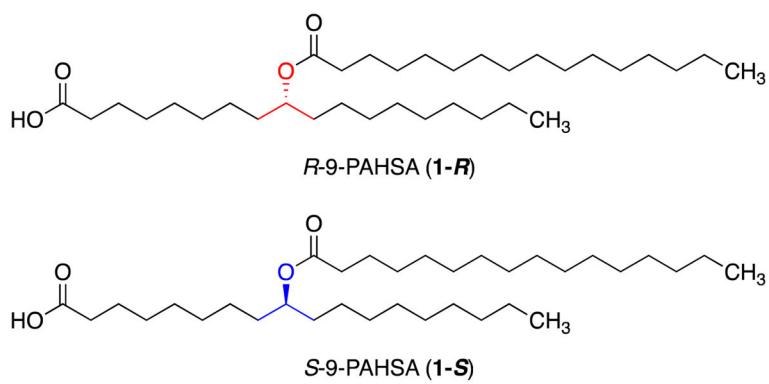


Figure 2.
S-9-PAHSA (**1-S**) and *R*-9-PAHSA (**1-R**).

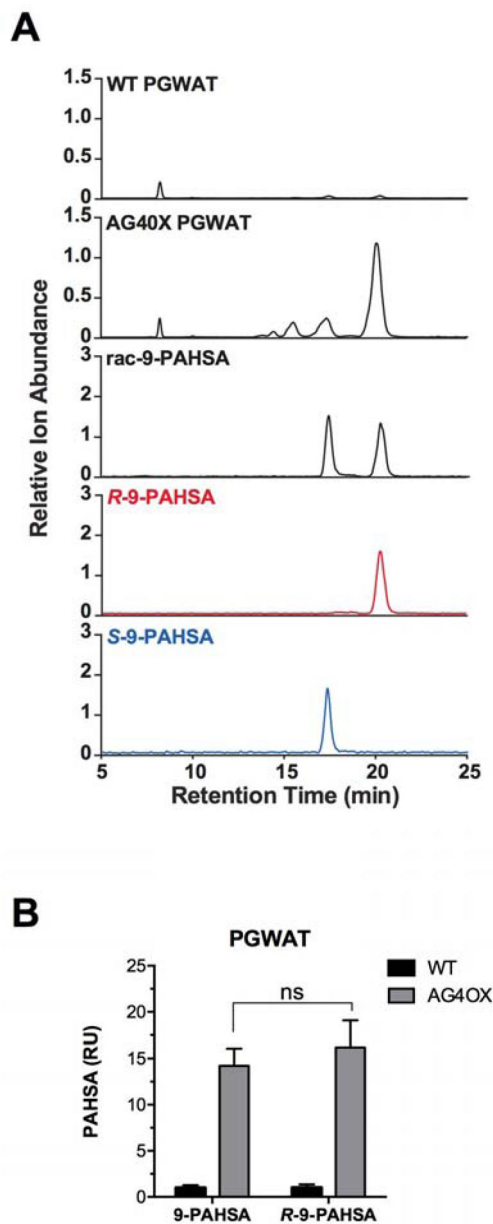


Figure 3.

R-9-PAHSA is the prominent enantiomer in mouse adipose tissue. (a) Representative PAHSA MS traces in PGWAT of WT and AG4OX mice with *rac*-, *R*-, and *S*-9-PAHSA standards resolved on a Lux 3 μ m Cellulose-3 chiral column. (b) 9-PAHSA and *R*-9-PAHSA fold change in AG4OX PGWAT vs WT PGWAT analyzed on a reversed-phase column and chiral column, respectively. PAHSA levels were normalized to the endogenous lipid d18:1/16:0 ceramide. Data represent means \pm the standard error of the mean for three biological replicates. ns, not significant.

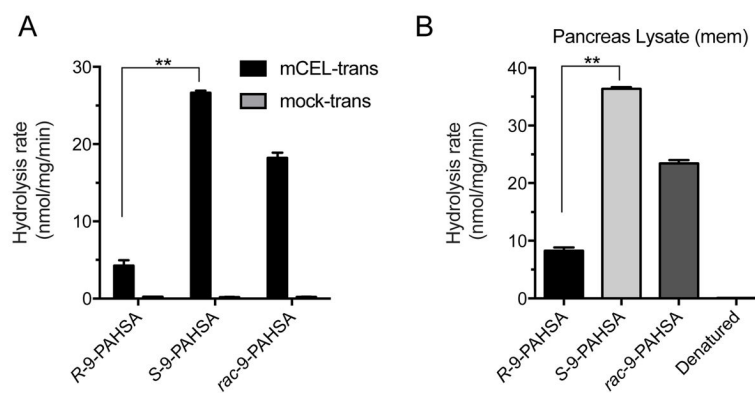


Figure 4. CEL prefers *S*-9-PAHSA as a substrate. (a) *R*-, *S*-, and *rac*-9-PAHSA hydrolysis activity for membrane lysates from CEL-transfected and mock-transfected HEK293T cells. Data represent means and the standard deviation for two biological replicates. (b) *R*-, *S*-, and *rac*-9-PAHSA hydrolysis activity for mouse pancreatic membrane lysates. Data represents mean and the standard error of the mean for three biological replicates. ** $p < 0.01$ by Student's *t* test.

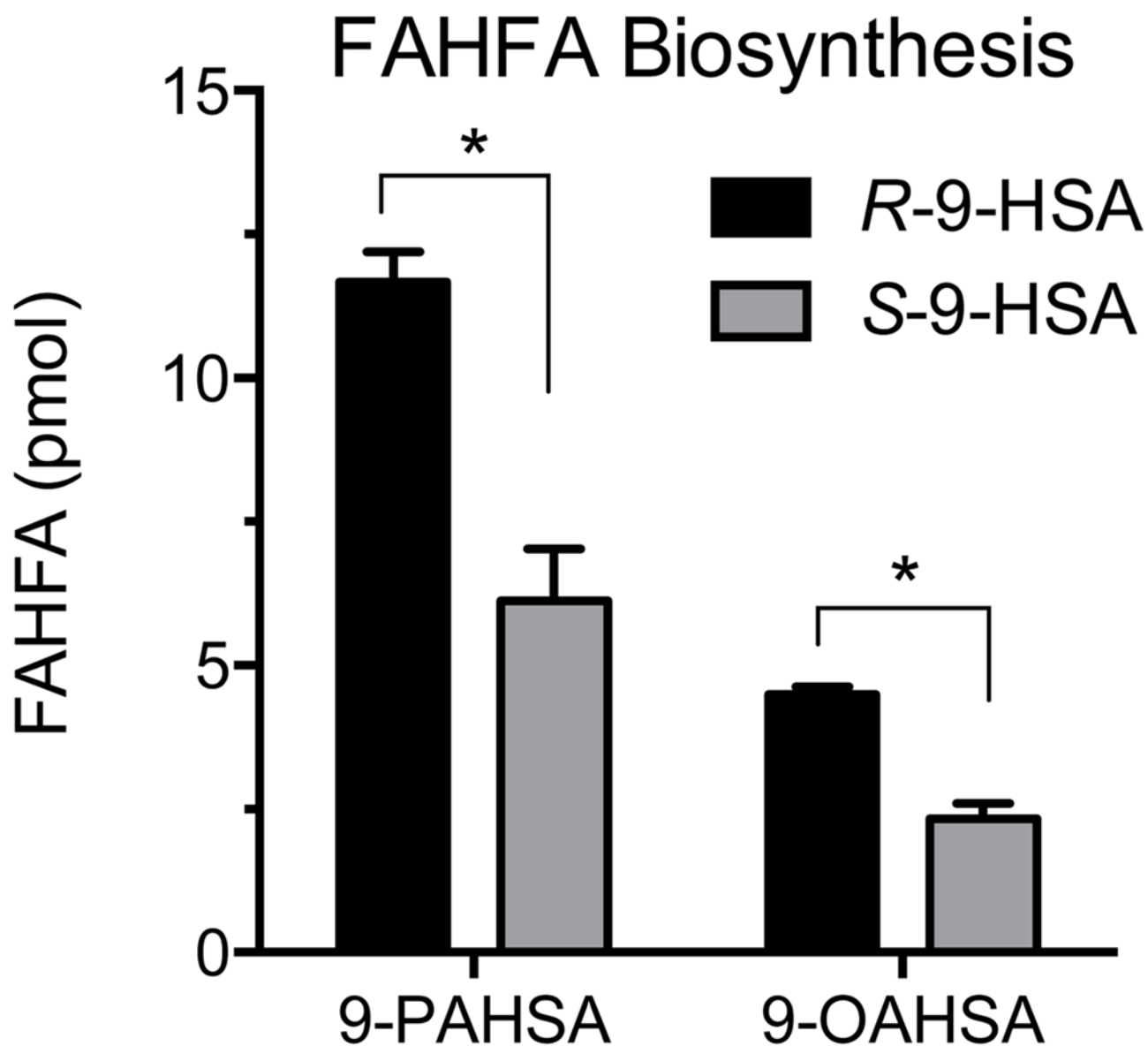
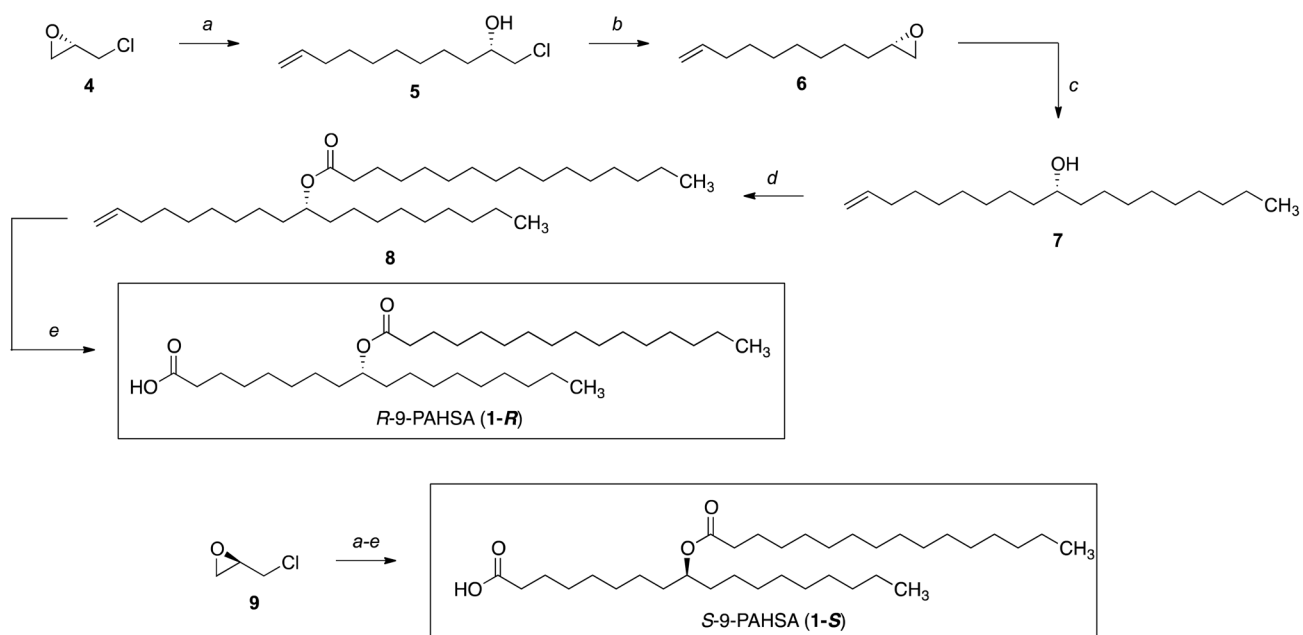


Figure 5. *R*-9-HSA is the preferred 9-HSA enantiomer for FAHFA biosynthesis. Biosynthesis of 9-PAHSA and 9-OAHSA in HEK293T cells after incubation with 100 μ M of *R*- or *S*-HSA for 2 h. * $p < 0.05$ by two-sided Student's *t*-test comparing *R*-9-HSA-treated versus *S*-9-HSA-treated HEK293T cells.

**Scheme 1.**

Syntheses of *R*-9-PAHSA from *S*-(+)-epichlorohydrin (**4**) and *S*-9-PAHSA from *R*-(+)-epichlorohydrin (**9**). Conditions: (a) 7-octenylmagnesium bromide, CuI, THF, -78 to 23 °C (**1-R** sequence 92%, **1-S** sequence 91%); (b) NaOH, Et₂O, 23 °C; (c) octylmagnesium chloride, CuI, Et₂O, -78 to 23 °C (**1-R** sequence 70%, **1-S** sequence 90%; over two steps); (d) palmitoyl chloride, pyr., CH₂Cl₂, 0 to 23 °C (**1-R** sequence 91%, **1-S** sequence 78%); (e) O₃, NMO, CH₂Cl₂, -10 °C then NaClO₂, NaH₂PO₄, 2-methyl-2-butene, *t*-BuOH, 23 °C (**1-R** sequence 94%, **1-S** sequence 96%).